Association of the I_γ and I_δ Charge Movement with Calcium Release in Frog Skeletal Muscle

Chiu Shuen Hui
Department of Cellular and Integrative Physiology, Indiana University Medical Center, Indianapolis, Indiana

ABSTRACT Charge movement and calcium transient were measured simultaneously in stretched frog cut twitch fibers under voltage clamp, with the internal solution containing 20 mM EGTA plus added calcium and antipyrylazo III. When the nominal free $[Ca^{2+}]_i$ was 10 nM, the shape of the broad I_γ hump in the ON segments of charge movement traces remained invariant when the calcium release rate was greatly diminished. When the nominal free $[Ca^{2+}]_i$ was 50 nM, which was close to the physiological level, the I_γ humps were accelerated and a slow calcium-dependent I_δ component (or state) was generated. The peak of ON I_δ synchronized perfectly with the peak of the calcium release rate whereas the slow decay of ON I_δ followed the same time course as the decay of calcium release rate. Suppression of calcium release by TMB-8 reduced the amount of Q_δ concomitantly but not completely, and the effects were partially reversible. The same simultaneous suppression effects were achieved by depleting the sarcoplasmic reticulum calcium store with repetitive stimulation. The results suggest that the mobility of Q_δ needs to be primed by a physiological level of resting myoplasmic Ca^{2+}. Once the priming is completed, more I_δ is mobilized by the released Ca^{2+} during depolarization.

INTRODUCTION

When charge movement was measured in cut fibers equilibrated with 10–20 mM EGTA in the end-pool solution, prominent I_γ humps appeared in the ON segments of charge movement traces (Horowicz and Schneider, 1981; Hui and Chandler, 1990, 1991; Hui, 1990, 1991a,b; Chen and Hui, 1991a,b; Hui and Maylie, 1991; Csernoch et al., 1991; Garcia et al., 1991a,b; Pizarro et al., 1991; Hui and Chen, 1992a,b, 1994a,b, 1995; Jong et al., 1995; Pape et al., 1996; Francini et al., 2001; Pape and Carrier, 2002). Even with 3 mM EGTA, Vergara and Caputo (1983) were able to record charge movement traces with relatively prominent I_γ humps. However, although a high concentration of EGTA facilitates the study of the I_γ hump, it reduces the resting free $[Ca^{2+}]$ in the myoplasm to far below the physiological level. We therefore removed practically all the EGTA in the end-pool solution, keeping only 0.1 mM to chelate any contaminating Ca^{2+} in the solution, so that charge movement could be measured under conditions close to the physiological state of the fiber. We found that, under this condition, Q_γ was very much reduced (Hui and Chen, 1997) and the associated I_γ hump was much less resolvable. This finding is interesting because it explains a longstanding mystery of why the I_γ hump was not present in charge movement traces published by some investigators (Kovacs et al., 1979; Melzer et al., 1986; Rios and Brum, 1987; Rios and Pizarro, 1988; Brum et al., 1988; Feldmeyer et al., 1990; Simon and Hill, 1992).

With the diminution of Q_γ in a fiber exposed to an extremely low $[EGTA]_i$, the total charge, Q_{total}, in the fiber appeared to be reduced. It is now clear that the reduction in Q_{total} was an artifact created by the pulse protocol and the baseline correction procedure that had been employed traditionally to record and analyze the signal. Specifically, the pulse duration was too short and insufficient length of the OFF segment of the current trace was digitized, leading to the truncation of the ON and OFF segments. When the lengths of both segments were increased, a new component of charge movement lasting hundreds of milliseconds became apparent (Hui, 1998). This new charge movement component depends on the presence of Ca^{2+} in the myoplasm. It was named I_δ and its associated charge was named Q_δ. With the presence of Q_δ, Q_{total} is actually increased rather than decreased in low $[EGTA]_i$.

The appearance of the I_δ component raised some important questions. First, is I_δ related to I_γ? One possibility is that Q_γ and Q_δ are entirely unrelated distinct charge entities, i.e., the decrease in Q_γ and the appearance of Q_δ are independent of each other. This was shown to be not the case by Pape et al. (1996), who reported a slowing of the kinetics of I_γ caused by the feedback of calcium release. One can then extend their observation to postulate that Q_γ could be converted to Q_δ. In other words, Q_γ and Q_δ belong to the same charge entity but are manifestations of different kinetic states that depend on the level of free $[Ca^{2+}]_i$. However, I found that, under the conditions of my experiments, even if all the Q_γ was converted to Q_δ, there was insufficient Q_γ to account for the large amount of Q_δ (see Table 2 and associated text in Discussion). Thus, some additional Q_δ is apparently mobilized by depolarization when the free $[Ca^{2+}]_i$ is restored to the physiological level. Even if the first part of Q_δ shares the same origin as Q_γ, the additional part might not. If so, how are I_γ

Submitted June 23, 2004, and accepted for publication October 29, 2004.

Address reprint requests to Dr. Chiu Shuen Hui, Dept. of Cellular and Integrative Physiology, Indiana University Medical Center, 635 Barnhill Dr., Indianapolis, IN 46202. Tel.: 317-274-8238; Fax: 317-274-3318; E-mail: cshui@iupui.edu.

0006-3495/05/02/1030/16 $2.00

doi: 10.1529/biophysj.104.048215

and I_δ associated with calcium release? The experiments reported in this article were aimed at providing some answers to the latter question. It was found that the results from the experiments are consistent with the idea that Q_γ could be the trigger for calcium release and part of Q_δ could be generated by the release. Thus, the longstanding controversy between the ''trigger hypothesis'' and the ''feedback hypothesis'' for Q_γ might have been resolved. The information concerning whether Q_γ and Q_δ belong to the same charge entity or are separate distinct charge species will be presented in the Discussion. Because of the complexity of Q_δ, a complete answer to this question is still unavailable.

METHODS

Solutions

Solutions are given in Table 1. In solutions *B–D*, Cs^+ was used to suppress K^+ currents. In solutions *E–H*, TEA^+ and Rb^+/Cs^+ were used to suppress K^+ currents and tetrodotoxin was used to block Na^+ current. External solutions *G* and *H* were used to enable the application of long TEST pulses. To avoid the activation of the slow inward Ca^{2+} current, all the Ca^{2+} was replaced by Mg^{2+}. TEA-Cl and TEA-OH were bought from R.S.A. Corp. (Ardsley, NY). TEA-CH_3SO_3 was prepared by titrating methanesulphonic acid (Aldrich, Milwaukee, WI) with TEA-OH. TEA-gluconate was prepared by titrating gluconic acid lactone (Sigma, St. Louis, MO) with TEA-OH. Cesium creatine phosphate was prepared from sodium creatine phosphate (Calbiochem, La Jolla, CA) by an ion exchange procedure that we have used in many published works (starting with Chandler and Hui, 1990, and Hui and Chandler, 1990). Special care was taken to minimize the amount of contaminating calcium introduced by the ion exchange procedure (Hui, 1998). With 20 mM EGTA in the internal solution, the amount of free Ca^{2+} was estimated to be $<10^{-12}$ M. With either 0.4 or 1.8 mM total added calcium, the nominal free $[Ca^{2+}]_i$ was estimated to be ~10 nM in solution *B* and ~50 nM in solutions *C* and *D*. The latter value is assumed to be close to the physiological level. Antipyrylazo III (ApIII) was bought from ICN K & K Laboratories, Plainview, NY, and dissolved in the internal solution. 8-(*N*,*N*-diethylamino)octyl 3,4,5-trimethoxybenzoate hydrochloride (TMB-8) was purchased from Calbiochem and the appropriate amount was dissolved directly in the external solution.

Muscle and fiber preparation

All experiments were performed on cut twitch fibers from English frogs, *Rana temporaria*, cold acclimated in a refrigerator at ~4°C. In accordance with a procedure approved by the Institutional Animal Care and Use Committee, animals were killed by decapitation and destruction of the brain and spinal cord. The procedure for dissecting and mounting cut fibers from semitendinosus muscle was similar to that used by Kovacs et al. (1983) and Irving et al. (1987). Cut fiber segments were dissected in solution A. A stretched fiber segment was mounted in a double Vaseline-gap chamber. To facilitate the entry of the calcium indicator ApIII into the myoplasm, the outer membranes of the fiber in the end pools were permeabilized by a 2-min exposure to 0.01% saponin (Sigma). The beginning of the treatment marked time zero of an experiment. After the proper internal and external solutions were introduced, the voltage clamp was turned on at about the 20th–23rd minute, and the fiber was repolarized. The fiber was allowed to recover for ~30 min during which various ions diffused into the myoplasm in the center-pool region. The temperature of the center-pool solution was kept at 13–14°C.

Data acquisition

The instrumentation for data acquisition was designed and fabricated by the Biomedical Instrumentation Laboratory of Yale Department of Cellular and Molecular Physiology. Ten analog signals were connected to the input channels of the module. They included six optical signals (see below), three electrical signals, and the temperature. The electrical signals were the potential in one end pool (V_1), the potential in the other end pool (V_2), and the total current injected into the latter end pool (I_2). The cutoff frequency of

TABLE 1 Solutions

	Relaxing solution				
	Potassium glutamate	$MgSO_4$	K_2-EGTA	K_2-Pipes	
A	120	1	0.1	5	
	End-pool or internal solutions				
	Cesium glutamate	Cs_2-CP	$MgSO_4$	Cs_2-EGTA	Cs_2-ATP	Cs_2-PEP	Mg-ATP	Cs-MOPS	Total Ca^{2+}
B	42.5	20	0	20	0	0	5.5	20	0.4
C	42.5	20	0	20	0	0	5.5	20	1.8
D	50	20	6.8	20	5.5	5	0	5	1.8
	Center-pool or external solutions								
	TEA-Cl	TEA-CH_3SO_3	TEA-gluc	RbCl	Cs_2SO_4	$CaCl_2$	$Ca(CH_3SO_3)_2$	$Mg(CH_3SO_3)_2$	$MgSO_4$
E	120	-	-	2.5	-	1.8	-	-	-
F	-	115	-	-	5	-	2	-	-
G	-	100	-	-	5	-	-	10	-
H	-	-	110	-	-	-	-	-	10

All concentrations are in mM. Pipes, piperazine-N,N′-bis[2-ethane sulphonic acid; CP, creatine phosphate; PEP, phospho(enol)pyruvate; MOPS, 3-(*N*-morpholino) propanesulphonic acid; TEA, tetraethylammonium; CH_3SO_3, methanesulphonate; and gluc, gluconate. Internal solutions B–D contained 5 mM glucose. Solution C was used in earlier experiments. In later experiments, solution C was replaced by solution D, in which 20 mM MOPS was replaced by 5 mM PEP and 5 mM MOPS (Pape et al., 1995). There was no detectable difference between the results obtained with the two solutions, within experimental errors. External solutions E–H contained 1 μM tetrodotoxin and 5 mM MOPS. Relaxing and internal solutions were titrated to pH 7.0 with KOH and CsOH, respectively. External solutions were titrated to pH 7.1 with TEA-OH. The osmolarities of internal and external solutions were adjusted to 235 mOsm (Godt and Maughan, 1988).

the eight-pole Bessel filter in each channel was set at 0.6 kHz. Data was digitized at a rate of 10 μs per point and sent to a PDP 11/73 computer for processing. The points in each channel were compressed before storage. As a result, each point in a stored trace corresponds to 1 ms. Multiplexing of the channels was arranged in a way to synchronize the compressed points in all the channels in time.

Charge movement measurement

Holding potential was set at −90 mV. Control pulses were applied from −110 mV to the holding potential and test pulses from the holding potential to the potentials desired. The condition of the fiber was tracked by monitoring the holding current throughout an experiment. Subsequent data analysis included linear cable analysis of the control records. The analysis yielded information about myoplasmic resistance (r_i), membrane resistance (r_m), membrane capacitance (c_m), and gap factor of the Vaseline seals defined by $r_e/(r_e + r_i)$ (Chandler and Hui, 1990). The terms r_e and r_i represent the external and internal resistance per unit length of the fiber underneath the Vaseline seals. Each $I_{control}$ trace was an average of four sweeps and all I_{test} traces were single-sweep. Each charge movement measurement is displayed as an $I_{test} - I_{control}$ trace, which is obtained by subtracting a scaled $I_{control}$ trace from a paired I_{test} trace.

To estimate the amount of Q_δ in a charge movement trace, the procedure developed in Hui (1998) was applied to the OFF segment of the trace. The first step was to correct for the baseline. Each OFF segment was fitted by a sum of two exponentials and a sloping straight line, with the fastest phase of decay being excluded from the fit. For comparison, the fitting was repeated by replacing the sloping straight line with a constant. In principle, in the presence of a nonlinear time-dependent ionic current, such as a changing leakage current underneath the Vaseline seals, fitting with a sloping straight line should be more accurate, whereas in the absence of such a current, both fitting methods should yield similar results if a sufficiently long baseline was recorded. As will be shown in Figs. 6 and 8, the latter turned out to be true in the experiments presented. The straight line or constant resulting from the fit was used for baseline correction and the longer time constant was used to represent the decay time constant τ_δ of the OFF I_δ component. An integration of the complete OFF transient yielded the OFF Q_{total}. The second step was to separate the OFF I_δ component from the OFF I_{total}. The OFF I_δ component was found to have a rising phase with a time constant τ_r (Hui, 1998). The waveform of the OFF I_δ component can thus be expressed as

$$-A\{1 - \exp(-t/\tau_r)\}\exp(-t/\tau_\delta). \quad (1)$$

An integral of this expression yielded the amount of OFF Q_δ.

Optical measurement

The experimental procedure and processing of the optical records followed those of Irving et al. (1987) and Maylie et al. (1987a,b) and had been used in our previous work (Maylie and Hui, 1991; Hui, 1999). The optical system was built on an upright microscope (model ACM, Carl Zeiss, New York, NY). Optical measurements were made with a 55.5-μm diameter spot of light focused on the axis of the fiber segment located in the center-pool region. Since three wavelengths are required to accurately describe the calcium indicator signal in muscle (Baylor et al., 1982), the transmitted light was separated into three beams with two beam-splitting cubes. The beams were made quasimonochromatic by passing through three interference filters with peak transmission wavelengths at 550 nm (10-nm bandwidth), 720 nm (30 nm), and 810 nm (30 nm). Each beam was further split into two beams of linear polarizations (0° and 90° with respect to the fiber axis) with a polarizing beam-splitting cube.

The intensities of the six resulting beams were monitored with photodiodes (model UV-100B, EG&G Electro-Optics Div., Salem, MA) and fed to the inputs of the optical channels of the data acquisition module. Absorbance measurements were made with unpolarized incident light (mode 1 in Irving et al., 1987). The absorbance at each wavelength $A(\lambda)$ was computed from the 1:2 average of A_0:A_{90}. The intrinsic absorbance signal $\Delta A_i(810)$ was filtered by a 0.05-kHz digital Gaussian filter (Colquhoun and Sigworth, 1983). The procedures described in Maylie et al. (1987a) were used to subtract the contributions due to the intrinsic absorbance changes to yield the dye-related $\Delta A(720)$.

Computation of calcium release rate

In this article, calcium release rate (Rel) will be used to refer to the $d\Delta[Ca_T]/dt$ signal, in which Ca_T represents the total amount of calcium (free and bound) in the myoplasm. Rel was computed from the dye-related $\Delta A(720)$, based on a model similar to the one used by Baylor et al. (1983), but modified to include the binding of Ca^{2+} to EGTA in addition to its binding to ApIII, troponin, and parvalbumin. The following values were used for the parameters in the model: 2.55×10^4 M^{-1} cm^{-1} for $\varepsilon(550)$ of ApIII, 1.46×10^4 M^{-1} cm^{-1} for $\Delta\varepsilon(720)$ of the Ca-ApIII complexes, 3.4×10^{-8} M^2 for the apparent k_D between Ca^{2+} and ApIII, 240 μM for the total concentration of troponin, 0.575×10^8 M^{-1} s^{-1} and 115 s^{-1} for k_1 and k_{-1} of Ca^{2+} binding to troponin, 2 mM for the total concentration of parvalbumin, 1.25×10^8 M^{-1} s^{-1} and 0.5 s^{-1} for k_1 and k_{-1} of Ca^{2+} binding to parvalbumin, 3.3×10^4 M^{-1} s^{-1} and 3.0 s^{-1} for k_1 and k_{-1} of Mg^{2+} binding to parvalbumin, and 1.0×10^6 M^{-1} s^{-1} and 0.5 s^{-1} for k_1 and k_{-1} of Ca^{2+} binding to EGTA. Throughout this article, only the computed Rel traces will be shown. For a typical computation from the dye-related $\Delta A(720)$ traces to yield the free $[Ca^{2+}]$ traces, the $[Ca_T]$ traces, and finally the Rel traces, refer to Figs. 1 and 2 *A* of Hui (1999). The peak amplitude of Rel, represented by Rel_p, and the time-to-peak in each trace were determined by fitting the peak with a parabolic function.

RESULTS

Charge movement and calcium release in cut fibers with reduced myoplasmic Ca^{2+}

In measuring charge movement from cut fibers, the presence of 20 mM EGTA without added Ca^{2+} in the internal solution greatly enhanced the manifestation of the I_γ component as a prominent hump (see references in Introduction). Unfortunately, calcium transient cannot be monitored in these fibers with a metallochromic calcium indicator such as ApIII, presumably because most of the Ca^{2+} released from the sarcoplasmic reticulum (SR) is precluded from successful binding with ApIII by EGTA and the free $[Ca^{2+}]_i$ is too low to replenish the SR calcium store after activities. To enable the observation of calcium transient, the $[EGTA]_i$ has to be reduced, but when the concentration is lowered to 0.1 mM, the I_γ hump can hardly be resolved (Hui and Chen, 1997). The first experiment to be reported here is aimed at exploring whether there is any condition under which both prominent I_γ hump and sizable calcium transient can be recorded simultaneously. The rationale is that perhaps the 20 mM EGTA should be retained and it might be possible to partially restore the free $[Ca^{2+}]_i$ to a level just sufficient to enable the measurement of calcium transient without compromising the prominence of the I_γ hump.

Fig. 1 shows the results from an experiment of this kind. The fiber was bathed in a TEA-Cl external solution. By trial and error, it was found that the optimal free $[Ca^{2+}]_i$ was

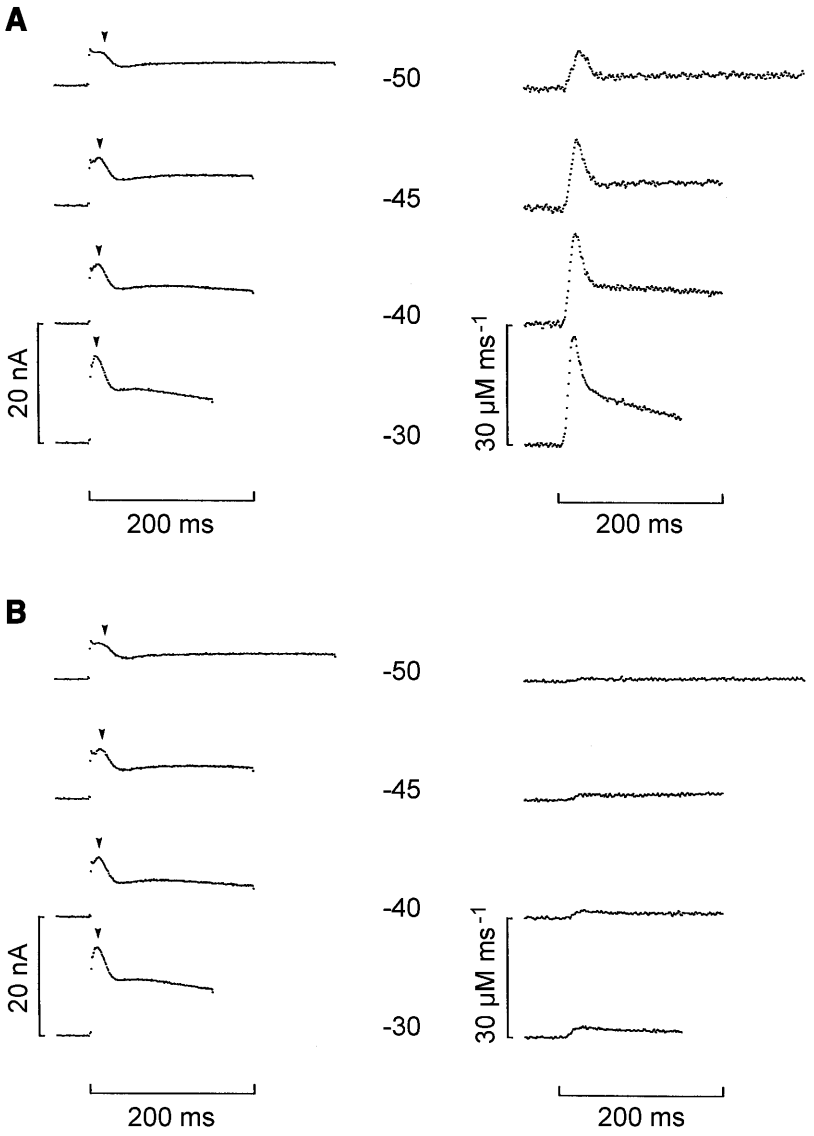

FIGURE 1 Invariance of I_γ when calcium release was reduced in a cut fiber. The end pools contained solution *B* and the center pool contained a TEA-Cl Ringer solution (solution *E*). From the beginning to the end of the experiment, the holding current changed from −27 to −34 nA and the gap factor decreased from 0.982 to 0.977. At the 56th minute, 0.66 mM ApIII was added to the end pools. In each panel, the left column shows the ON-segments of $I_{test} - I_{control}$ traces. Calcium release rate (Rel) was computed from corrected $\Delta A(720)$ signal as described in Methods and the traces are shown in the right column. Each pair of electrical and optical traces in the same row were taken simultaneously. The number in the middle of each row shows the potential in mV during the test pulse. (*A*) Representative traces taken from the 112th to the 120th minute, during which the myoplasmic [ApIII] increased from 0.72 to 0.83 mM. The values of Rel_p are 9.3, 17.0, 23.5, and 27.3 μM ms^{-1} at −50, −45, −40, and −30 mV, respectively. (*B*) Representative traces taken from the 147th to the 155th minute, during which the myoplasmic [ApIII] increased from 1.27 to 1.41 mM. The values of Rel_p are 1.2, 1.6, 2.2, and 2.7 μM ms^{-1} at −50, −45, −40, and −30 mV, respectively. Fiber diameter, 78 μm. Sarcomere length, 3.8 μm. The arrowheads mark the peaks of the I_γ humps.

~10 nM (solution *B*). A sequence of depolarizing pulses with amplitudes ranging from 10 to 90 mV were applied at 2-min intervals to elicit pairs of charge movement (*left column*) and Rel (*right column*) traces. Only the traces at intermediate depolarizations are shown in Fig. 1 *A* to reveal the prominent I_γ humps (as indicated by the *arrowheads*) in the electrical traces. Although the nominal free $[Ca^{2+}]_i$ was ~10 nM, the magnitudes of Rel were quite substantial in the early stage of the experiment. In this and the next four figures, only ON segments of the charge movement traces are shown for comparison with the Rel traces. The OFF segments are irrelevant as the inward charge movement had no correlation with the cessation of calcium release.

Another identical sequence of depolarizing pulses was applied almost half an hour later in the experiment and the pairs of traces in the same potential range are shown in Fig. 1 *B*. The Rel traces shown in the right column were very much reduced. From the values of Rel_p given in the figure legend, calcium release was reduced to ~10% of those in Fig.1 *A*. This diminution can be attributed to the insufficient replenishment of the SR calcium store after multiple large depolarizations (between the two sequences, not shown) because the free $[Ca^{2+}]_i$ was below the physiological level. In contrast to the reduction in Rel, a comparison of the charge movement traces in Fig. 1, *A* and *B*, showed that the I_γ humps remained unchanged between the two sequences of runs. The same invariance was observed in two other fibers in which the same experimental protocol was used. This reinforces our previous conclusion that I_γ cannot be generated by the feedback of calcium release from the SR.

The invariance in the shape of the I_γ hump reported here is different from the finding that repetitive stimulation slowed the kinetics of I_γ (Hui, 1991b) and that calcium release exerted feedback on the kinetics of I_γ (Jong et al., 1995; Pape et al.,

1996; Hui and Chen, 1997) but in agreement with the finding that the reduction of calcium transient by low concentrations of tetracaine had no influence on I_γ (Csernoch et al., 1988). It should be noted, however, that the experimental conditions employed in the various studies were different.

Another interesting relationship between I_γ and Rel is shown in Fig. 2. To facilitate the comparison of the time courses of I_γ and Rel, the format for displaying the traces in Fig. 1 *A* is changed such that each pair of traces is lined up in time, with the electrical trace directly above the optical trace. After the rearrangement, it became obvious that the peak of I_γ preceded the peak of Rel waveform at all potentials. The same observation was also reported by Csernoch et al. (1988).

This temporal relationship between I_γ and Rel might provide additional support for the above conclusion that I_γ cannot be generated by the feedback of calcium release. However, it should be noted that charge movement is a signal localized in the T-tubules whereas calcium transient is a global signal averaged over all regions of the sarcomeres illuminated by the light spot. Diffusion of the released Ca^{2+} from the triads to the A-bands should introduce some weighted delay in the global calcium transient. Thus, this temporal relationship between I_γ and Rel is not as definitive as the invariance of I_γ shown in Fig. 1 in supporting the conclusion.

Charge movement and calcium release in cut fibers with physiological level of myoplasmic Ca^{2+}

The effect of calcium release on charge movement was quite different when the free $[Ca^{2+}]_i$ was restored to the physiological level, as shown in Fig. 3. The traces shown in Fig. 3 were recorded from a fiber with the free $[Ca^{2+}]$ in the internal solution adjusted nominally to 50 nM (solution *C*). With the elevated free $[Ca^{2+}]_i$, it was anticipated that calcium-dependent Cl^- current would be activated during depolarization (Hui and Chen, 1994b) and complicate the analysis of charge movement traces. To avoid this problem, the Cl^- in the external solution was completely replaced with an impermeant anion. The traces shown in Fig. 3 were recorded from a fiber bathed in a TEA-CH_3SO_3 external solution. Between -55 and -35 mV, small and brief I_γ humps (indicated by *arrowheads*) after the first I_β peak can be visualized in the charge movement traces. The higher free $[Ca^{2+}]_i$ abbreviated the durations of the I_γ humps as compared with those in Fig. 2. This is consistent with the finding reported in Hui and Chen (1997). Fig. 2 *A* of that article showed specifically how I_γ evolved from a broad prominent hump that was well separated from I_β to a brief small hump that followed I_β closely when the free $[Ca^{2+}]_i$ was elevated. For a closer visualization of I_β and I_γ on an expanded timescale, refer to trace 6 or 7 of Fig. 2 *B* in that study. Based on the information provided by that figure, there should be no doubt that the small humps marked by the arrowheads in my Fig. 3 are I_γ.

A completely new feature that has never been observed in any charge movement trace before is the appearance of another slower hump after the I_γ hump. The late hump can be visualized in all the traces and can be aligned perfectly with the peak of the Rel waveform, as indicated by the dashed lines. One might argue that this late hump could be I_γ in the conventional sense, but it is impossible because I_γ should be accelerated when the resting free $[Ca^{2+}]_i$ is at a higher level and hence cannot peak later than that in the fiber of Fig. 2. However, it is possible that the late hump might reflect the flow of part of Q_γ that is transformed to a slow kinetic state, as reported by Pape et al. (1996). The late hump was observed in many other fibers in which the same experimental protocol was used, 61 in the same solution, 6 in sulfate, and 26 in gluconate. It is worth mentioning that the late hump

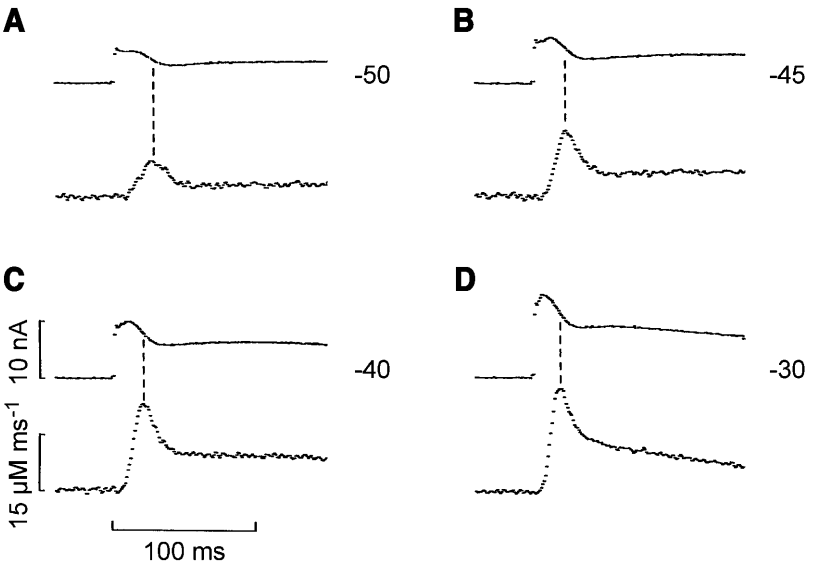

FIGURE 2 I_γ precedes the peak of Rel in a cut fiber. Same experiment as in Fig. 1. Each panel shows the ON segment of an $I_{test} - I_{control}$ trace (*top*) and a Rel trace (*bottom*) taken simultaneously. (*A–D*) Pairs of traces taken from the first to fourth row of Fig. 1 *A* and displayed in expanded timescale. The number to the right of each electrical trace shows the potential in mV during the test pulse.

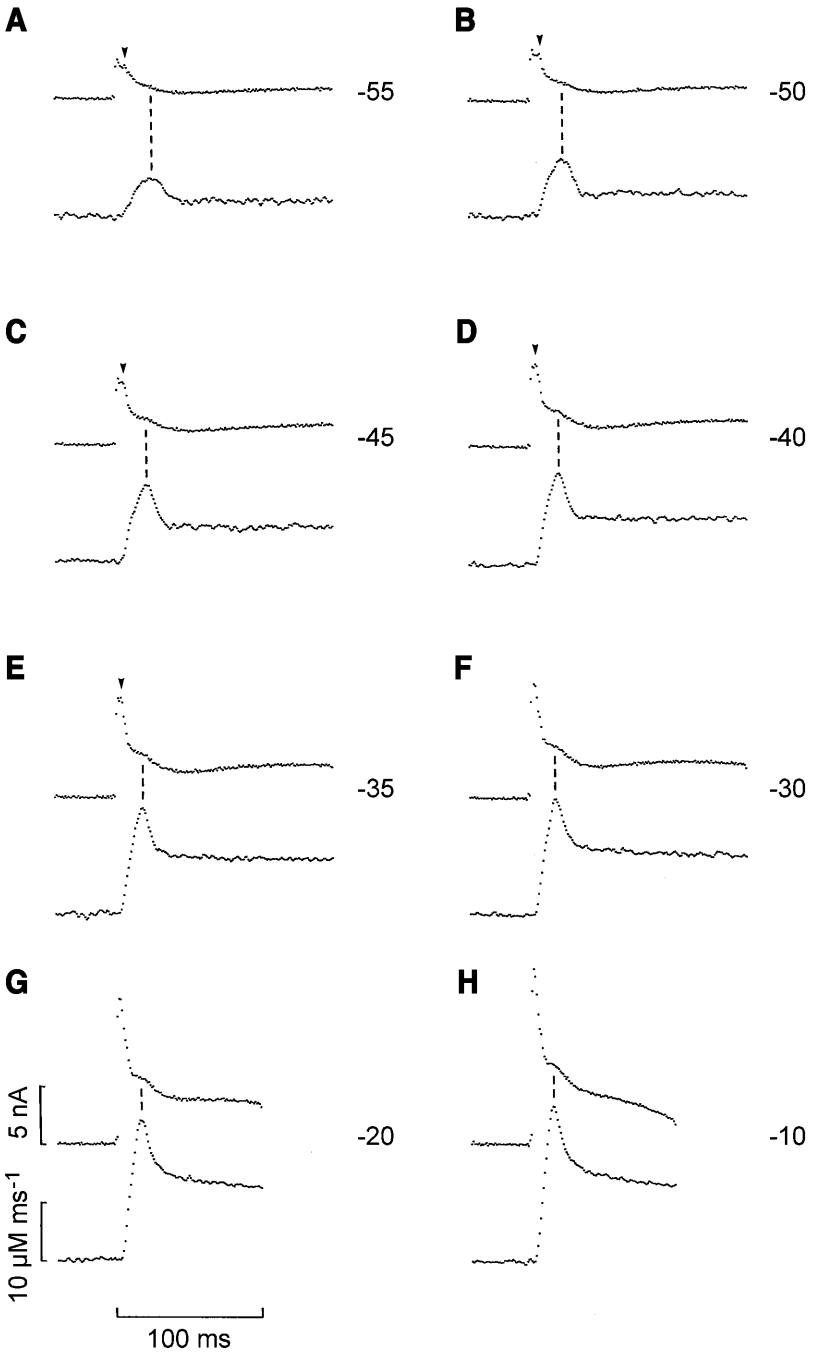

FIGURE 3 Temporal association of the peak of I_δ with that of Rel in a cut fiber. The end pools contained solution *C* and the center pool contained a TEA-CH_3SO_3 Ringer solution (solution *F*). From the beginning to the end of the experiment, the holding current changed from −48 to −50 nA and the gap factor decreased from 0.974 to 0.972. At the 49th minute, 0.65 mM ApIII was added to the end pools. At the 93rd minute the [ApIII] in the end pools was reduced to 0.29 mM. Each panel shows the ON segment of an $I_{test} - I_{control}$ trace (*top*) and a Rel trace (*bottom*) taken simultaneously. (*A–H*) Pairs of traces taken from the 105th to the 124th minute, during which the myoplasmic [ApIII] increased from 0.66 to 0.79 mM. Fiber diameter, 91 μm. Sarcomere length, 4 μm. The number to the right of each electrical trace shows the potential during the test pulse. The arrowheads mark the peaks of the I_γ humps.

was also observed in 42 fibers bathed in Cl^-. In those experiments, the late hump was not obscured by the calcium-dependent Cl^- current because the ionic current was activated quite slowly even at large depolarizations. All these results suggest that the late hump could be a genuine signal rather than an artifact and could be closely associated with calcium release because of their tight temporal relationship. It is thus hypothesized that the newly discovered late hump is the peak of the slow calcium-dependent component of charge movement that has been named I_δ (Hui, 1998). It should be emphasized that this peak of I_δ was not apparent in the traces of Figs. 1 and 2 when the free $[Ca^{2+}]_i$ was at an extremely low level.

Association of I_δ with calcium release

It was explained in Hui (1998) that to study the slow ON and OFF I_δ current, the durations of the ON and OFF segments of the charge movement traces should be sufficiently long to enable baseline fits. Consequently, a calcium-free external solution needs to be used to avoid the slow inward Ca^{2+} current. Fig. 4 shows three pairs of electrical and optical

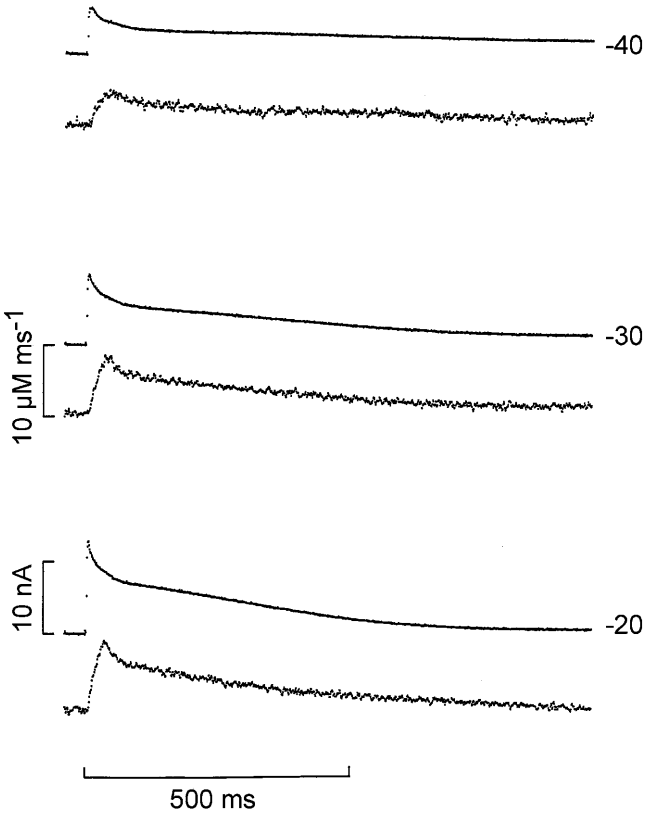

FIGURE 4 Temporal association of the slow decay of I_δ with that of Rel in a cut fiber. The end pools contained solution *D* and the center pool contained a calcium-free TEA-gluconate Ringer solution (solution *H*). From the beginning to the end of the experiment, the holding current changed from −34 to −36 nA and the gap factor remained unchanged at 0.981. At the 90th minute, ApIII was added to the end pools, but its concentration was not measured. The three pairs of traces shown were taken from the 203rd to the 212th minute, during which the myoplasmic [ApIII] increased from 0.58 to 0.64 mM. Each pair shows the ON segment of an $I_{test} - I_{control}$ trace (*top*) and that of a Rel trace (*bottom*) taken simultaneously. Fiber diameter, 96 μm. Sarcomere length, 4 μm. The number to the right of each electrical trace shows the potential in mV during the test pulse.

traces elicited by 2000-ms depolarizing pulses to −40, −30, and −20 mV. To increase the temporal resolution, only the first 1000 ms of the traces are shown in the figure. The slowly decaying I_δ components in the traces resembled those shown in Hui (1998). The application of long pulse and abolition of inward Ca^{2+} current facilitate the checking of ON-OFF charge equality. The checking procedure was presented in Fig. 5 of Hui (1998). The main feature in this figure is that the slow decays of I_δ and Rel shared similar time courses, although the waveforms of the two signals were not exactly identical. The same similarity was observed in 14 other fibers bathed in either a calcium-free TEA-CH_3SO_3 or calcium-free TEA-gluconate external solution. This suggests that the slow I_δ is closely associated with calcium release.

The magnitudes of the Rel in Fig. 4 were smaller than, and the peaks were not as sharp as, those shown in Fig. 3. The obscurity of the peak was not due to the use of gluconate, as it was also observed when $CH_3SO_3^-$ was used. The obscurity is universally true in all experiments employing long depolarizing pulses, which presumably deplete the calcium content of the SR more effectively. The employment of a calcium-free external solution might also contribute to the differences (Hui, 1999). Concomitantly, the slow humps that were observed in Fig. 3 were much more inconspicuous in Fig. 4. In fact, this is the strongest piece of supporting evidence that can be used to associate the slow hump with calcium release, other than the close temporal relationship between the two signals. Since I_δ is also closely associated with calcium release (Fig. 4), the slow hump could actually be part of I_δ, as hypothesized in the preceding section. It thus appears that I_δ contains a peak followed by a slow decay but the conditions for observing both parts are mutually exclusive. The long depolarizing pulses (in conjunction with a calcium-free external solution) that are required for the measurement of the slow decay phase of I_δ in Fig. 4 are not optimal for the detection of the peak of I_δ. On the other hand, Fig. 3 showed that prominent peaks of I_δ can be recorded by applying short depolarizing pulses, but under this condition, the decay phase of I_δ is truncated.

Concomitant suppression of I_δ and calcium release by TMB-8

To gain further support of the hypothesis that I_δ is associated with calcium release, two interventions were applied to reduce calcium release and investigate whether I_δ is affected concomitantly. In each intervention, the amount of Q_δ was compared with the magnitude of Rel_p as the experiment progressed. For the purpose of estimating the amount of Q_δ, the OFF segments of charge movement traces are much more useful than the ON segments, because the procedure that was developed to separate Q_δ from Q_{total} is only applicable to the OFF segments (see Methods). Hence, unlike Figs. 1–4 which show ON segments of charge movement traces, Figs. 5 and 7 show OFF segments instead.

According to Malagodi and Chiou (1974), TMB-8 inhibited contraction in skeletal muscle by suppressing calcium release. Since TMB-8 could serve as a useful agent for hindering the calcium release process (Janis et al., 1987), it was used in the first intervention. An experiment employing TMB-8 is shown in Fig. 5. Each pair of charge movement trace (in Fig. 5 *A*) and Rel trace (in Fig. 5 *B*) was elicited by a constant 150-ms pulse to −20 mV and recorded simultaneously. Although the short pulses truncated the ON charge movement, they were less damaging and so slowed the run-down of the fiber. Long (1800-ms) OFF segments of the charge movement traces were recorded to facilitate fitting of baselines. To increase temporal resolution, only 800 ms of the segments are shown in the figure. The pair of traces in the first row was taken before the application of TMB-8. A sizable OFF I_δ can be visualized in the charge movement trace after a very fast and a somewhat slower phase of decay, which

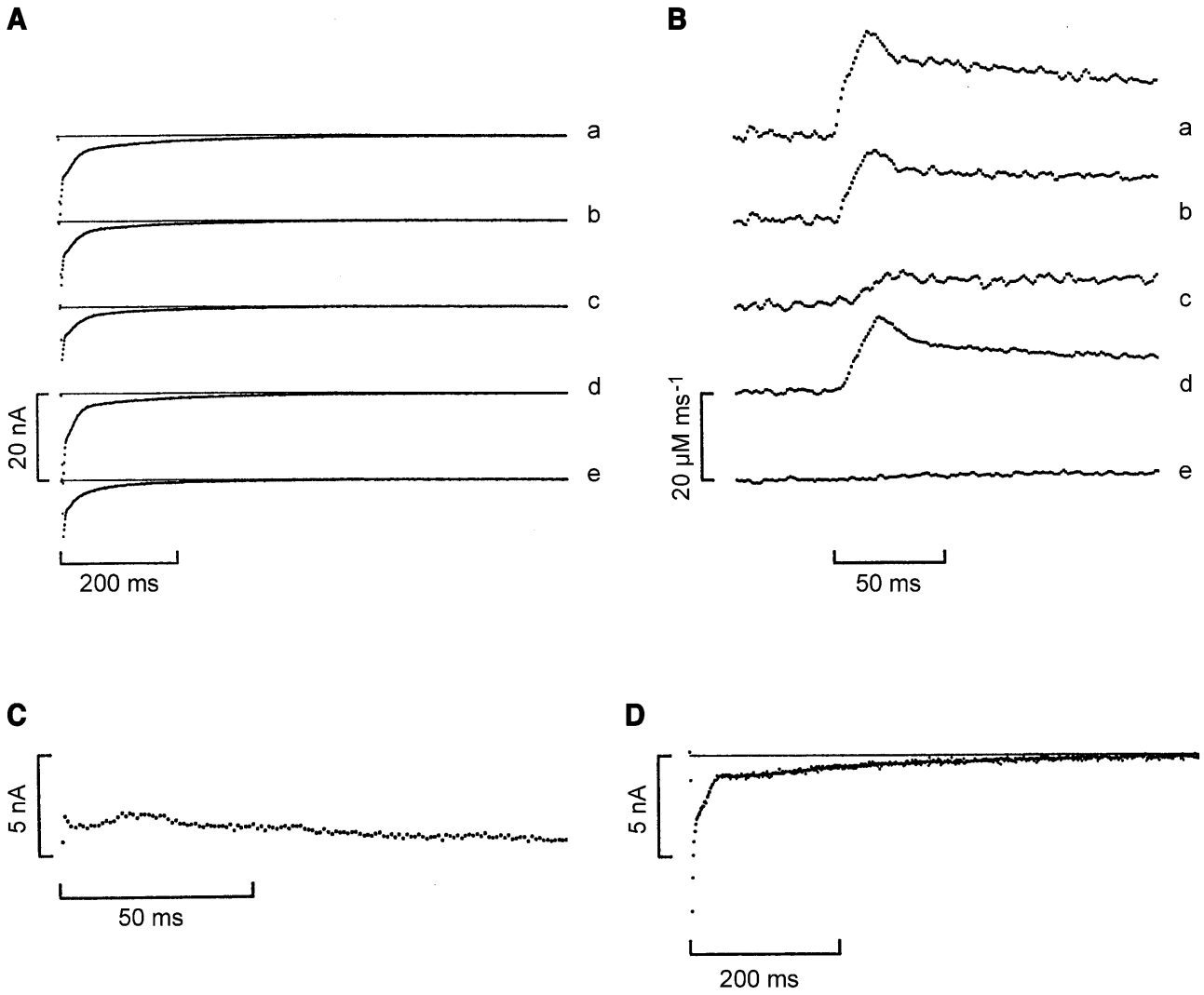

FIGURE 5 Effects of TMB-8 on charge movement and Rel in a cut fiber. The end pools contained solution *C* and the center pool contained a TEA-CH_3SO_3 Ringer solution (solution *F*). From the beginning to the end of the experiment, the holding current changed from −38 to −55 nA and the gap factor decreased from 0.975 to 0.965. At the 56th minute, 0.68 mM ApIII was added to the end pools. At the 108th minute the [ApIII] in the end pools was reduced to 0.21 mM. (*A*) OFF segments of $I_{test} - I_{control}$ traces. Only the early 800 ms of the segments are shown and the thin straight lines mark the zero-current axes. (*B*) Rel traces. Each pair of traces in the same row of *A* and *B* was elicited simultaneously by a 150-ms test pulse to −20 mV. The first pair of traces (*a*) was taken at the 129th minute when the myoplasmic [ApIII] was 0.46 mM. At the 131st minute, 60 μM TMB-8 was added to the center pool. The second and third pairs of traces (*b* and *c*) were taken at the 132nd and the 135th minute, during which the myoplasmic [ApIII] increased from 0.48 to 0.50 mM. At the 140th minute, the TMB-8 was washed out. The fourth pair of traces (*d*) was taken at the 152nd minute, when the myoplasmic [ApIII] was 0.59 mM. At the 173rd minute, 60 μM TMB-8 was added to the center pool again. The fifth pair of traces (*e*) was taken at the 180th minute, when the myoplasmic [ApIII] was 0.65 mM. (*C*) The ON counterpart of the difference trace shown in *D*. (*D*) Difference trace obtained by subtracting trace *c* from trace *a* in *A*. Fiber diameter, 89 μm. Sarcomere length, 4 μm.

presumably corresponded to the OFF I_β and I_γ components, respectively. The Rel trace showed an early peak.

The second pair of traces was taken 1 min after the application of 60 μM TMB-8 to the center pool. TMB-8 acted very fast. Within a minute, the OFF I_δ was reduced and the peak of Rel was suppressed. After another 3 min, the third pair of traces was taken. Both the OFF I_δ and the peak of Rel were further reduced. To examine the difference between the first and the third charge movement traces more closely, the difference trace is shown in Fig. 5 *D*. TMB-8 appeared to suppress all three components of OFF charge movement, but the dominating effect was on I_δ, as revealed by the sizable slow decay in the difference trace. The ON segment of the difference trace is also shown in Fig. 5 *C* for comparison. It has an I_δ hump that peaks at ~18 ms, more or less matching the peak of Rel in trace *a* of Fig. 5 *B*.

Another pair of traces (not shown) was taken before TMB-8 was washed out. The fourth pair of traces in the figure was taken 12 min after washout. Both the slow I_δ component and the Rel waveform recovered appreciably but not completely, implying that the effect of TMB-8 was reversible, at least partially. Subsequently, TMB-8 was reapplied. The fifth pair

of traces showed that calcium release was completely suppressed by then, but the slow I_δ component was only partially reduced.

To differentiate the effect of TMB-8 on the slow I_δ component from that on the fast I_β and I_γ components, the amount of OFF Q_δ was estimated from each charge movement trace shown in Fig. 5 (and others not shown) by the procedure described in Methods. The baseline was first corrected by fitting with a sum of two exponentials and a sloping straight line. Since the rising time constant τ_r was not measured in this fiber, it was adopted from the average value obtained from other fibers. As shown in Hui (1998), the value was 8.2 ms. An integration of Expression 1 with this value of τ_r yielded the values of OFF Q_δ, which are plotted as solid diamonds in Fig. 6 *A*. Finally, the difference between each OFF Q_{total} and OFF Q_δ gave the sum of the OFF Q_β and Q_γ, which is plotted as an open square in Fig. 6 *A*. No attempt was made to separate Q_β and Q_γ and their sum will be referred to as $Q_{\beta\gamma}$ from here on. For comparison, the value of Rel_p was estimated from each optical trace and is plotted in Fig. 6 *B*.

The values of Q_δ, $Q_{\beta\gamma}$, and Rel_p estimated from the first pair of traces in Fig. 5 *A* (marked by the letter *a* in Fig. 6, *A* and *B*), namely 51.3 nC μF^{-1}, 17.0 nC μF^{-1}, and 24.2 $\mu M\ ms^{-1}$, were used as control. The *left shaded area* in each panel indicates the first application of TMB-8. At the instant the third pair of traces was recorded (marked by *c*), TMB-8 had suppressed Q_δ and Rel_p to 47 and 32% of control, respectively. TMB-8 was not without effect on $Q_{\beta\gamma}$ but the reduction was much smaller, to 73% of control. This agrees with Fig. 5 *D*. Since the amount of charge is normalized by the membrane capacitance, there was concern that the reduction in the amount of charge could be caused by an increase in membrane capacitance. Fig. 6 *C* is shown to clarify this point. The membrane capacitance did increase slightly at the instant the third pair of traces was taken (it was 110% of control), but the increase was not large enough to account for the decrease in $Q_{\beta\gamma}$ and definitely far too small to account for the even larger decrease in Q_δ. After washout (indicated by the *white area* in each panel between the two *shaded areas*), the data marked by *d* showed that Q_δ and Rel_p recovered hand in hand to 77 and 71% of control, whereas $Q_{\beta\gamma}$ recovered almost fully to 98% of control. At that time, membrane capacitance returned halfway to 106% of control. The second application of TMB-8 (indicated by the *right shaded area*) completely suppressed Rel_p but reduced Q_δ and $Q_{\beta\gamma}$ to 37 and 76% of control (data marked by *e*) whereas the membrane capacitance was increased to 114% of control.

The amounts of Q_δ and $Q_{\beta\gamma}$ were also estimated by fitting the OFF segment of each charge movement trace with a sum of two exponentials and a constant. The values for Q_δ are plotted in Fig. 6 *A* as solid circles, which show exactly the same pattern of change as the solid diamonds when TMB-8 was applied and washed out. The values for $Q_{\beta\gamma}$ are not shown because they are extremely close to the values represented by the open squares. The values represented by the solid circle and the solid diamond from the same charge movement trace differ by ~9 nC μF^{-1}, on average. These small differences suggest that the sloping baselines obtained with the first method of fitting are essentially horizontal, i.e., not much different from the constant baselines obtained with the second method of fitting. This similarity can only be achieved with sufficient duration of the OFF segments, namely 1800 ms in the experiment shown in Figs. 5 and 6 (and similar experiments).

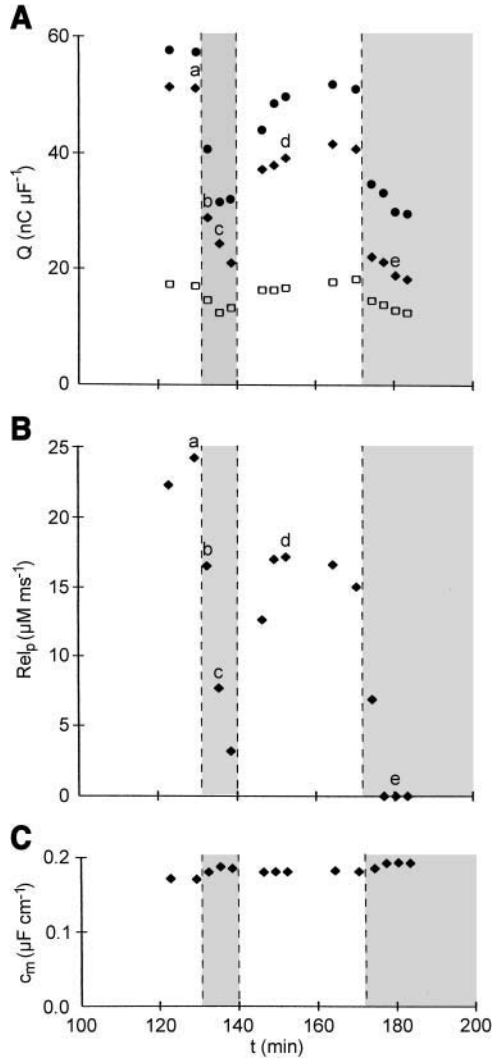

FIGURE 6 Concomitant suppression of I_δ and peak Rel by TMB-8. Same experiment as in Fig. 5. All values in the plot were obtained from $I_{test} - I_{control}$ traces or Rel traces elicited by test pulses to −20 mV. (*A*) Open squares and solid symbols represent $Q_{\beta\gamma}$ and Q_δ, respectively, estimated from the OFF segments of $I_{test} - I_{control}$ traces and were separated by the procedure described in Methods. Solid circles and diamonds were obtained by fitting the OFF segment with a sum of two exponentials and a constant and with a sum of two exponentials and a sloping straight line, respectively. The lettered points were obtained from traces shown in Fig. 5 *A*. (*B*) Rel_p estimated from Rel traces. The lettered points were obtained from traces shown in Fig. 5 *B*. (*C*) Linear membrane capacitance estimated from control current traces, which were elicited from −110 to −90 mV.

The main points of Fig. 6 are: first, the effect of TMB-8 on Rel correlates better with its effect on Q_δ than that on $Q_{\beta\gamma}$; second, when calcium release is completely suppressed by TMB-8, part of Q_δ still remains mobile. Similar results were obtained from five other fibers that were exposed to 60–100 μM TMB-8. When calcium release was suppressed to a negligible level, Q_δ was reduced to 53 $\pm$ 5 (S.E.M.) % of control at a potential of -30 to -20 mV, averaged over all six fibers. The reversibility of the effects of TMB-8 was examined in three of the other five fibers. In two of them, TMB-8 was washed out after 40–45 min of exposure and neither fiber could release calcium any more. In the third fiber, TMB-8 was applied for 10 min and Rel_p was down to 27% of control. On washout, Rel_p recovered to 67%. In the experiment shown in Figs. 5 and 6, the first exposure lasted only 9 min, which was sufficient to suppress Rel_p to $<$10% of control. Even with exposures as short as 9–10 min, the recovery of Rel_p after washout was incomplete. It might be possible to achieve complete recovery if exposure was much shorter.

Concomitant suppression of I_δ and calcium release by repetitive stimulation

Another intervention to reduce the amount of Ca^{2+} released from the SR is to reduce the supply of Ca^{2+} inside the store. This can be accomplished by stimulating the fiber repetitively to deplete the Ca^{2+} store, and, obviously, long pulses are more effective for this purpose. This approach was used in the experiment shown in Fig. 7. The fiber was bathed in a calcium-free TEA-CH_3SO_3 external solution. Each pair of charge movement trace (in Fig. 7 *A*) and Rel trace (in Fig. 7 *B*) was elicited by a 2000-ms TEST pulse to -30 mV. Only 5 of the 13 pairs of traces taken are shown in the figure. Some other pairs of traces taken at other potentials are also not shown. The first pair of traces (*a*) was taken when calcium release was fairly typical and served as control. After three other stimulations (traces not shown), the second pair of traces (*b*) was taken. By then the peak amplitude of the Rel trace was already down to less than half of the control, indicating that the SR store was emptied quite effectively. When the fifth pair of traces (*e*) was taken, calcium release was barely noticeable and the slow I_δ component was reduced. To examine the difference between the first and fifth charge movement traces more closely, the difference trace is shown on an expanded scale in Fig. 7 *C*. It shows the reduction of I_δ as well as of $I_{\beta\gamma}$.

Following the analysis shown in Fig. 6, the amounts of $Q_{\beta\gamma}$ and Q_δ were estimated from the charge movement traces shown in Fig. 7 (and others not shown). The amounts of OFF Q_δ estimated from the integral of Expression 1, after fitting the OFF segments with a sum of two exponentials and a sloping straight line, are plotted as solid diamonds in Fig. 8 *A*. The amounts of OFF $Q_{\beta\gamma}$ obtained from the differences between OFF Q_{total} and OFF Q_δ are plotted as open squares in the same panel. The corresponding values of Rel_p were calculated from the Rel traces and are plotted in Fig. 8 *B*.

The values of Q_δ, $Q_{\beta\gamma}$, and Rel_p estimated from the first pair of traces in Fig. 7 *A* (marked by the letter *a* in Fig. 8, *A* and *B*), namely 58.4 nC μF^{-1}, 17.1 nC μF^{-1}, and 21.2 μM ms^{-1}, served as control. At the instant the second pair of traces was taken (marked by *b*), partial depletion of the SR calcium store reduced Q_δ to 69% of control and Rel_p to 41% of control. The $Q_{\beta\gamma}$ was hardly affected: it was reduced to 95% of control. The SR calcium store was more depleted at the end of the experiment. Q_δ, $Q_{\beta\gamma}$, and Rel_p were reduced to 53, 89, and 10% of control (marked by *e*). Throughout the experiment, the membrane capacitance was decreasing slightly instead of increasing as in Fig. 6 *C*. Its value when the fifth pair of traces was taken was 94% of control.

As in Fig. 6 *A*, the estimation of the amounts of Q_δ was repeated by fitting the OFF segment of each charge movement trace with a sum of two exponentials and a constant. The values are plotted in Fig. 8 *A* as solid circles. They differ from the values represented by the solid diamonds by $\sim$7 nC μF^{-1}, on average. With this baseline fitting, the residual amount of Q_δ at the end of the experiment (marked by *e*) was 54% of control, which is practically the same as the 53% obtained with the former fitting.

Similar experiments were performed on two other fibers. In one fiber, Q_δ, $Q_{\beta\gamma}$, and Rel_p were reduced to 62, 90, and 16% of control. In the other fiber, the quantities were reduced to 52, 86, and 8%, respectively. The results, together with those from Fig. 8, show that calcium release can be reduced effectively by depleting the SR calcium store. They strongly support the conclusions drawn in the preceding section that the reduction of calcium release correlates with a reduction of Q_δ (with much less change in $Q_{\beta\gamma}$) and that when calcium release is greatly reduced, a portion of Q_δ still remains mobile. On the one hand, calcium depletion is a preferable intervention because it avoids the suspicion of any undesirable secondary pharmacological effect exerted by TMB-8, such as its effect on $Q_{\beta\gamma}$. On the other hand, by the time the SR calcium store is successfully depleted, reversibility is very difficult to achieve. Also, complete depletion of the SR calcium store may never be achieved unless an ATPase inhibitor is used in conjunction with repetitive stimulation.

DISCUSSION

Association of Q_γ with calcium release

When a muscle fiber is depolarized, movement of voltage sensors in tetradic dihydropyridine receptors (DHPRs) triggers the release of Ca^{2+} from the SR. In principle, some of the released Ca^{2+} should bind to transverse tubule membranes and result in a potential change, which should in turn activate the movement of more voltage sensors. Dr. W. K. Chandler was the first to consider this feedback effect, as referenced in Horowicz and Schneider (1981) and Hui

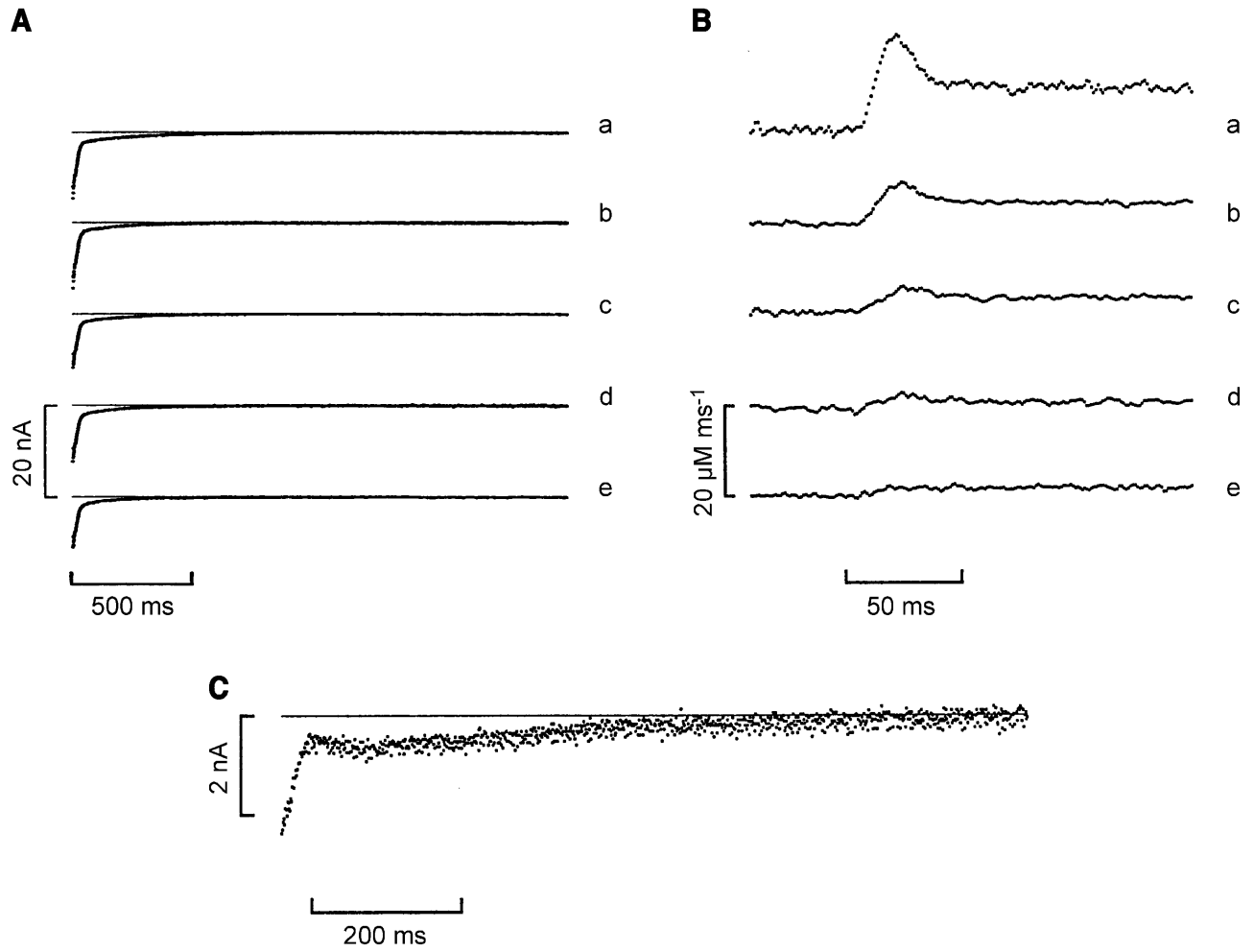

FIGURE 7 Effects of repetitive stimulation on charge movement and Rel in a cut fiber. The end pools contained solution *D* and the center pool contained a calcium-free TEA-CH_3SO_3 Ringer solution (solution *G*). From the beginning to the end of the experiment, the holding current changed from −25 to −37 nA and the gap factor decreased from 0.986 to 0.982. At the 63rd minute, ApIII was added to the end pools but its concentration was not measured, and at the 123rd minute, some ApIII was removed from both end pools. (*A*) OFF segments of $I_{test} - I_{control}$ traces. The thin straight lines mark the zero-current axes. (*B*) Rel traces. Each pair of traces in the same row was elicited simultaneously by a 2000-ms test pulse to −30 mV. The five pairs of traces were taken at the 173rd, 192nd, 215th, 235th, and 260th minutes when the myoplasmic [ApIII] increased from 0.49 to 0.64 mM and the linear membrane capacitance decreased slightly from 0.166 to 0.156 μF cm^{-1}. (*C*) Expanded difference trace obtained by subtracting trace *e* from trace *a* in *A*. Fiber diameter, 89 μm. Sarcomere length, 4 μm.

(1983). That led to the proposal that Q_γ is generated by this feedback (Pizarro et al., 1991; Shirokova et al., 1994). This has been referred to as the ''feedback hypothesis'' for Q_γ. However, results in this article showed that Q_γ cannot be generated by the feedback of released Ca^{2+} (also supported by Jong et al., 1995; Chawla et al., 2002; Squecco et al., 2003). First, when calcium release is reduced to a negligible level, the waveform and size of I_γ remain unaltered (Fig. 1; see also Csernoch et al., 1988). Second, the chronological order of the peaks of I_γ and Rel precludes the possibility of Q_γ being a consequence of calcium release (Fig. 2; see also Csernoch et al., 1988). However, the second evidence is not as definitive as the first (see text associated with Fig. 2).

If Q_γ is not a consequence of calcium release, and since it is closely associated with calcium release (Huang, 1982; Hui, 1982; Vergara and Caputo, 1983), then it is quite likely that Q_γ is a trigger for calcium release. This supports the ''trigger hypothesis'' for Q_γ and resolves the controversy between the ''trigger hypothesis'' and ''feedback hypothesis''. If so, the positive feedback of calcium release on charge movement mentioned in the preceding paragraph is missing. The slow I_δ can fill the gap, as will be explained below.

Waveform of I_δ

When charge movement is measured in a cut fiber containing a physiological level of free $[Ca^{2+}]_i$, a slowly decaying current was observed in the ON and OFF segments of the traces. The capacitive nature of this slow current was established in the preceding article (Hui, 1998). Specifically,

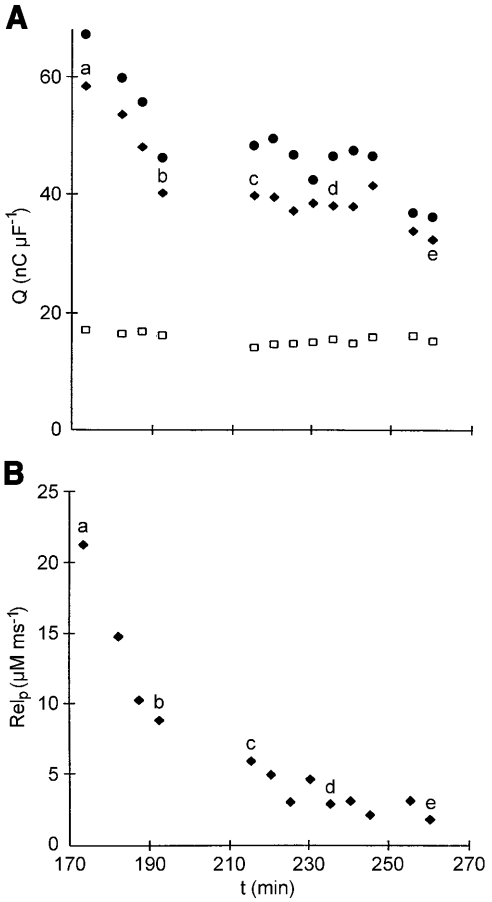

FIGURE 8 Concomitant suppression of I_δ and peak Rel by repetitive stimulations. Same experiment as in Fig. 7. All values were obtained from $I_{test} - I_{control}$ traces or Rel traces elicited by test pulses to −30 mV. (*A*) Open squares and solid symbols represent $Q_{\beta\gamma}$ and Q_δ, respectively, estimated from the OFF segments of $I_{test} - I_{control}$ traces and were separated by the procedure described in Methods. Solid circles and diamonds were obtained by fitting the OFF segment with a sum of two exponentials and a constant and with a sum of two exponentials and a sloping straight line, respectively. The lettered points were obtained from traces shown in Fig. 7 *A*. (*B*) Rel_p estimated from Rel traces. The lettered points were obtained from traces shown in Fig. 7 *B*.

the possibility that the current arises as a result of permeation of cations or anions through the outer membranes was ruled out. The current was called the I_δ component of charge movement. Experiments were also performed to determine the waveform of the OFF I_δ component in an attempt to develop a method for separating Q_δ from the Q_{total}. It was found that OFF I_δ has a slow rising phase with a time constant of the order of 10 ms and the amount of Q_δ is much larger than the combined amount of Q_β and Q_γ. The ON I_δ should also have a slow rising phase but its time constant varies as a function of the potential during depolarization, making it difficult to separate the ON Q_δ from the ON Q_{total}

In the experiments presented in this article, the ON I_δ component was studied in greater detail to gain information about the relationship between I_δ and calcium release. Although the exact shape of the rising phase of ON I_δ is still not known with certainty, it appeared that ON I_δ consists of a peak (Fig. 3) and a slow decay phase (Fig. 4), quite similar in shape to the Rel waveforms computed from absorbance signals recorded at the same time. Thus, in the ON segment of a charge movement trace, the peaks of I_γ and I_δ are manifested as the early and late humps, respectively, after the fast I_β peak (Fig. 3).

It should be noted that the conditions optimal for the observation of the peak and the slow decay of ON I_δ are mutually exclusive. The observation of the slow phase of ON I_δ necessitates the use of long depolarizing pulses (Fig. 4), which makes the peaks in Rel and ON I_δ much less conspicuous. These peaks are most prominent when measured with short depolarizing pulses (Fig. 3), which truncate the slow decay of ON I_δ. Because of this, it is difficult to establish the capacitive nature of the late hump, as baseline correction cannot be carried out with short pulses and ON-OFF charge equality cannot be verified. Hence, the only piece of evidence used to support the inclusion of the late hump as part of I_δ (which is a capacitive current) is its presence when the Rel trace shows a sharp peak (Fig. 3) and its absence when the Rel trace does not show a sharp peak (Fig. 4). Combining the results from both groups of experiments, it can be postulated that the waveform of ON I_δ has the same shape as that of Rel.

Existence of I_δ requires physiological level of free $[Ca^{2+}]_i$

The presence of a sharp peak in the Rel trace does not guarantee the appearance of the peak of ON I_δ. Fig. 2 shows that when the free $[Ca^{2+}]_i$ was a small fraction of the normal physiological amount, the peak of ON I_δ could not be detected. Another peculiar feature of the traces is that the I_γ humps were still broad and prominent as if the acceleration of I_γ kinetics observed by Jong et al. (1995), Pape et al. (1996), and Hui and Chen (1997) did not occur, or occurred to a much lesser extent.

One possible explanation for these observations is that perhaps the mobilization of Q_δ and the conversion of Q_γ to Q_δ in response to calcium release require initial priming by some resting Ca^{2+} in the myoplasm. The resting concentration has to be close to the physiological level and the priming time course is quite slow. Thus, when the resting concentration is below the physiological level, such as 10 nM in the case of Figs. 1 and 2, even a sizable calcium release for a brief period of time could not exert much effect on the I_γ hump nor mobilize any Q_δ because there was not sufficient time for the priming to take place during the brief elevation of free $[Ca^{2+}]_i$. The peculiar features in Fig. 1 were captured at just the appropriate resting free $[Ca^{2+}]_i$. Had the resting free $[Ca^{2+}]_i$ been lower, Rel might be too small to be detected with ApIII. Had the resting free $[Ca^{2+}]_i$ been higher, the

shape of the I_γ hump most likely would not be invariant when Rel was diminished.

Association of Q_δ with calcium release

One might argue that the similarity between the waveforms of I_δ and Rel could be a coincidence. To establish the association of Q_δ with calcium release more firmly, two interventions were applied to interfere with calcium release and to observe how Q_δ is affected. The first intervention made use of an intracellular calcium antagonist TMB-8, which has been used widely as a pharmacological tool for inhibiting calcium release from stores inside a variety of cell types (for review, see Janis et al., 1987). According to Malagodi and Chiou (1974), TMB-8 inhibited contraction in skeletal muscle by suppressing calcium release. Fig. 6 shows that when calcium release was blocked by TMB-8, Q_δ was reduced concomitantly, and if TMB-8 was washed out promptly, both calcium release and Q_δ were restored in parallel. The reversibility of the blockades supports the association of Q_δ with calcium release quite convincingly. Unfortunately, the utilization of TMB-8 was not without flaw. The most serious concern is the reduction in $Q_{\beta\gamma}$ when Q_δ was reduced. Nonetheless, it is quite likely that the apparent decrease in $Q_{\beta\gamma}$ was caused by some other complications unrelated to calcium release, as discussed next.

First, the amounts of Q_β and Q_γ could decrease progressively over the course of the experiment as a result of fiber run-down which was inevitable. Fortunately, the restoration of $Q_{\beta\gamma}$ after washout of TMB-8 indicated that the decrease could not be entirely due to run-down. Second, the amounts of $Q_{\beta\gamma}$ and Q_δ extracted from each charge movement trace relied heavily on the method used to separate the charge components in the OFF segment. Since the time constant of the rising phase of OFF I_δ was not measured in the experiment of Fig. 6, the value 8.2 ms was adopted from the mean time constant from other fibers and used in Expression 1 to estimate the amount of Q_δ. This could introduce some error in the amount of Q_δ, and thus some error in the amount of $Q_{\beta\gamma}$ (see also Discussion in Hui, 1998). However, the difference trace in Fig. 5 *D* that was obtained from raw data shows that some reduction of $Q_{\beta\gamma}$ is real. Third, like most pharmacological agents, TMB-8 appeared to exert undesirable side effects on the fiber. TMB-8 at least increased the membrane capacitance slightly (Fig. 6 *C*), suggesting that TMB-8 has the ability to affect membrane electrical properties. This effect was unrelated to a change in calcium release, because a reduction in calcium release without TMB-8 in the experiment of Fig. 8 decreased the membrane capacitance instead. If so, there is no reason to expect that TMB-8 cannot affect Q_β and Q_γ directly, although to a relatively minor extent. In fact, the nature of multiple actions of TMB-8 has been noticed by some investigators (for example, Himmel and Ravens, 1990). Nonetheless, the parallel trend of diminution and reversible restoration of Q_δ and calcium release in response to the presence and washout of TMB-8 should establish, at least qualitatively, the association of Q_δ with calcium release without doubt.

The second intervention is presented in Figs. 7 and 8. The experiment showed that calcium release can be reduced without the use of any pharmacological agent by stimulating the fiber repetitively to deplete the SR calcium store. The results showed that when calcium release was reduced progressively from the beginning to the end of the experiment, the amount of Q_δ was reduced concomitantly. Although reversibility could not be demonstrated in the experiment, the side effect of the pharmacological approach was avoided and the results provide further support on the association of Q_δ with calcium release.

Complexities of Q_δ

Calcium release from the SR appears to slow the movement of Q_γ (Pape et al., 1996; Hui and Chen, 1997), suggesting that some Q_δ could actually be Q_γ converted to a different kinetic isoform, as suggested by Huang (1996). If all Q_δ were converted from Q_γ by calcium release, then a blockade of the release should simply stop the conversion without affecting the amount of charge moved. Pape et al. (1996) showed in one elegant experiment that when the resting free $[Ca^{2+}]_i$ of that fiber was changed from the physiological level to a negligible level, the amount of charge was conserved (see their Fig. 6 *B*). However, there exists a wealth of information from published works documenting that the amount of charge could be quite diversified at the two different levels of resting free $[Ca^{2+}]_i$.

Table 2 lists the values of Q_{max} for various charge components as well as the total charge in cut fibers containing 20 mM internal EGTA. The data from various sources shows that the amounts of total charge measured in fibers containing a negligible level of free $[Ca^{2+}]_i$ (in group *A*) is far less than those measured in fibers containing a physiological level of free $[Ca^{2+}]_i$ (in group *B*). With $CH_3SO_3^-$, the ratio is 1:6 (Hui, 1991b, versus Hui, 1998). With gluconate, the ratio is 1:2 (Jong et al., 1995, versus Pape et al., 1996) or 1:6 (Hui and Chen, 1995, versus author's unpublished data). With SO_4^{2-}, the ratio is 1:2 (Horowicz and Schneider, 1981, versus Hui, 1998) or 1:1 (Hui and Chandler, 1990, versus Hui, 1998). With Cl^-, the OFF I_δ can be revealed only when the calcium-activated Cl^- tail current is eliminated (Fig. 6 of Hui, 1998) but the amount of total charge in fibers containing a physiological level of free $[Ca^{2+}]_i$ has not been determined. It should be noted that the experimental conditions in different studies could be quite different. One important difference is the composition of solutions employed in various studies. In addition, the shorter duration of the depolarizing pulses used in group *A* studies might truncate some of the ON charge. Nonetheless, since 20 mM EGTA without added Ca^{2+} suppresses the

TABLE 2 Q_{max} values associated with various charge components

Major external Anion	Pulse duration	Q_β	Q_γ	$Q_{\beta\gamma}$	Q_δ	Q_{total}	Reference
A. 20 mM internal EGTA with no added Ca^{2+}							
SO_4^{2-}	100					26.3	Horowicz and Schneider (1981)
Cl^-	200	10.6	13.2			23.8	Hui and Chandler (1990)
SO_4^{2-}	400	36.4	11.8			48.2	Hui and Chandler (1990)
Cl^-	100-400	3.0	12.9			15.9	Chen and Hui (1991a)
Cl^-	100-400	9.9	10.2			20.1	Chen and Hui (1991b)
Cl^-	400	11.0	12.6			23.6	Hui (1991a)
$CH_3SO_3^-$	100-400	9.7	10.0			19.7	Hui (1991b)
Cl^-	400	12.4	11.4			23.8	Hui and Maylie (1991)
Cl^-	100-400	10.0	13.5			23.5	Hui and Chen (1992a)
Cl^-	200-400	10.5	13.1			23.6	Hui and Chen (1992b)
Gluconate	100-800					33.5	Jong et al. (1995)
Cl^-	100-400	13.1	11.1			24.2	Hui and Chen (1995)
Gluconate	100-400	1.6	9.7			11.3	Hui and Chen (1995)
B. 20 mM internal EGTA with added Ca^{2+}							
Gluconate	700-800					66.6	Pape et al. (1996)
SO_4^{2-}	2000			10.6	37.8	48.4	Hui (1998)
$CH_3SO_3^-$	2000			16.9	106.0	122.9	Hui (1998)
Gluconate	2000			10.5	56.0	66.5	Author's unpublished data

This table compares the best fit values of Q_{max} obtained by fitting a single Boltzmann function or a sum of two Boltzmann functions to Q-V plots. Only studies on cut fibers with 20 mM internal EGTA are included. Column 1 lists the major external anion used in each study. Column 2 gives the durations (in ms) of the depolarizing pulses. When a range of durations is listed in an entry, the variation was due to either changes in durations from fiber to fiber or changes in durations for different depolarizations in the same fiber, with decreasing duration for increasing depolarization. Columns 3–6 give the average best fit values (in nC μF^{-1}) of Q_{max} for various charge components. Column 7 gives either the average best fit values (in nC μF^{-1}) for the total charge or the sums of values from preceding columns. Column 8 gives the article references from which the values were retrieved. In Group *A*, the internal solution contained negligible resting free $[Ca^{2+}]_i$. In Group *B*, the resting free $[Ca^{2+}]_i$ was adjusted to approximately physiological level. The fibers in Chen and Hui (1991a) contained exceptionally small amounts of Q_β intrinsically. In Hui and Chen (1995), gluconate reduced the amount of Q_β in the fibers.

slow Q_δ, the shorter pulse durations should not make such drastic difference. Thus, a portion of Q_δ remains unaccounted for.

It was speculated in Hui (1998) that the unaccounted portion of Q_δ could be generated by calcium release. The association of Q_δ with Rel described here is in qualitative agreement with the speculation. However, when calcium release was reduced to a negligible level, a substantial amount of Q_δ could still be mobilized on depolarization (Figs. 6 and 8), which can be explained by at least two possibilities. First, when Ca^{2+} ions are released from the RyRs, they might be able to diffuse through some restricted space to reach the DHPRs without binding to EGTA or ApIII and are therefore undetected. Second, maybe some basal amount of I_δ, shown in the bottom trace of Fig. 7 *A*, is indeed not generated by calcium release but by the mere presence of resting Ca^{2+} in the myoplasm. Feedback of calcium release might convert some Q_γ to Q_δ to contribute more I_δ. Additionally, feedback of calcium release might mobilize more Q_δ to contribute even more I_δ.

Significance of Q_δ

At present, a likely scenario of the ensemble of charge is that Q_β consists collectively of gating charges of fast kinetics ion channels and Q_γ consists primarily of voltage sensors in tetradic DHPRs (since the gating charges of sodium channels should be inactivated by the time Q_γ is activated). The high threshold charge component, Q_h, described by Shirokova et al. (1995) and Francini et al. (2001) was probably not involved much in this study because the voltage range employed was ≤ -20 mV. This leaves the Ca^{2+} feedback on charge movement missing and the description of charge movement incomplete. The situation is remedied by the discovery of Q_δ, which could fill the missing gap. Since Q_γ triggers calcium release, it is logical to deduce that Q_δ is generated by Ca^{2+} feedback. Thus, Q_γ and Q_δ could, but do not necessarily have to, originate from the same pool of charge and are manifested in different phases of charge movement. The Q_δ generated by feedback should trigger more calcium release, which should generate more Q_δ, and so forth. Recently, Pape et al. (2002) showed evidence of how released Ca^{2+} could exert positive feedback on DHPRs to trigger more calcium release. The DHPRs and calcium release channels could therefore be involved in a progressive positive feedback loop mediated through Ca^{2+}, but the loop should converge rapidly because the movement of Q_δ should saturate. A combination of I_β, I_γ, and I_δ indeed has the potential to complete the description of the ensemble of charge movement components.

This project was supported by a grant from the National Institutes of Health (NS21955).

REFERENCES

Baylor, S. M., W. K. Chandler, and M. W. Marshall. 1982. Optical measurements of intracellular pH and magnesium in frog skeletal muscle fibres. *J. Physiol.* 331:105–137.

Baylor, S. M., W. K. Chandler, and M. W. Marshall. 1983. Sarcoplasmic reticulum calcium release in frog skeletal muscle fibres estimated from arsenazo III calcium transients. *J. Physiol.* 344:625–666.

Brum, G., R. Fitts, G. Pizarro, and E. Rios. 1988. Voltage sensors of the frog skeletal muscle membrane require calcium to function in excitation-contraction coupling. *J. Physiol.* 398:475–505.

Chandler, W. K., and C. S. Hui. 1990. Membrane capacitance in frog cut twitch fibers mounted in a double Vaseline-gap chamber. *J. Gen. Physiol.* 96:225–256.

Chawla, S., J. N. Skepper, and C. L.-H. Huang. 2002. Differential effects of sarcoplasmic reticular Ca^{2+}-ATPase inhibition on charge movements and calcium transients in intact amphibian skeletal muscle fibres. *J. Physiol.* 539:869–882.

Chen, W., and C. S. Hui. 1991a. Existence of Q_γ in frog cut twitch fibers with little Q_β. *Biophys. J.* 59:503–507.

Chen, W., and C. S. Hui. 1991b. Differential blockage of charge movement components in frog cut twitch fibres by nifedipine. *J. Physiol.* 444:579–603.

Colquhoun, D., and F. J. Sigworth. 1983. Fitting and statistical analysis of single-channel records. *In* Single-Channel Recording. B. Sakmann and E. Neher, editors. Plenum Press, New York. 191–263.

Csernoch, L., C. L.-H. Huang, G. Szucs, and L. Kovacs. 1988. Differential effects of tetracaine on charge movements and Ca^{2+} signals in frog skeletal muscle. *J. Gen. Physiol.* 92:601–612.

Csernoch, L., G. Pizarro, I. Uribe, M. Rodriguez, and E. Rios. 1991. Interfering with calcium release suppresses I_γ, the delayed component of intramembranous charge movement in skeletal muscle. *J. Gen. Physiol.* 97:845–884.

Feldmeyer, D., W. Melzer, and B. Pohl. 1990. Effects of gallopamil on calcium release and intramembrane charge movements in frog skeletal muscle fibres. *J. Physiol.* 421:343–362.

Francini, F., C. Bencini, C. Piperio, and R. Squecco. 2001. Separation of charge movement components in mammalian skeletal muscle fibres. *J. Physiol.* 537:45–56.

Garcia, J., A. J. Avila-Sakar, and E. Stefani. 1991a. Differential effects of ryanodine and tetracaine on charge movement and calcium transients in frog skeletal muscle. *J. Physiol.* 440:403–417.

Garcia, J., G. Pizarro, E. Rios, and E. Stefani. 1991b. Effect of the calcium buffer EGTA on the ''hump'' component of charge movement in skeletal muscle. *J. Gen. Physiol.* 97:885–896.

Godt, R. E., and D. W. Maughan. 1988. On the composition of the cytosol of relaxed skeletal muscle of the frog. *Am. J. Physiol.* 254:C591–C604.

Himmel, H. M., and U. Ravens. 1990. TMB-8 as a pharmacological tool in guinea pig myocardial tissues. II. Effects of TMB-8 on membrane currents in isolated ventricular cardiomyocytes. *J. Pharmacol. Exp. Ther.* 255:300–304.

Horowicz, P., and M. F. Schneider. 1981. Membrane charge movement in contracting and non-contracting skeletal muscle fibres. *J. Physiol.* 314:565–593.

Huang, C. L.-H. 1982. Pharmacological separation of charge movement components in frog skeletal muscle. *J. Physiol.* 324:375–387.

Huang, C. L.-H. 1996. Kinetic isoforms of intramembrane charge in intact amphibian striated muscle. *J. Gen. Physiol.* 107:515–534.

Hui, C. S. 1982. Pharmacological dissection of charge movement in frog twitch muscle fibers. *Biophys. J.* 39:119–122.

Hui, C. S. 1983. Differential properties of two charge components in frog skeletal muscle. *J. Physiol.* 337:531–552.

Hui, C. S. 1990. D600 binding sites on voltage-sensors for excitation-contraction coupling in frog skeletal muscle are intracellular. *J. Muscle Res. Cell Motil.* 11:471–488.

Hui, C. S. 1991a. Comparison of charge movement components in intact and cut twitch fibers of the frog: effects of stretch and temperature. *J. Gen. Physiol.* 98:287–314.

Hui, C. S. 1991b. Factors affecting the appearance of the hump charge movement component in frog cut twitch fibers. *J. Gen. Physiol.* 98:315–347.

Hui, C. S. 1998. A slow calcium-dependent component of charge movement in *Rana temporaria* cut twitch fibres. *J. Physiol.* 509:869–885.

Hui, C. S. 1999. Calcium release in frog cut twitch fibers exposed to different ionic environments under voltage clamp. *Biophys. J.* 77:2123–2136.

Hui, C. S., and W. K. Chandler. 1990. Intramembranous charge movement in frog cut twitch fibers mounted in a double Vaseline-gap chamber. *J. Gen. Physiol.* 96:257–297.

Hui, C. S., and W. K. Chandler. 1991. Q_β and Q_γ components of intramembranous charge movement in frog cut twitch fibers. *J. Gen. Physiol.* 98:429–464.

Hui, C. S., and W. Chen. 1992a. Separation of Q_β and Q_γ charge components in frog cut twitch fibers with tetracaine: critical comparison with other methods. *J. Gen. Physiol.* 99:985–1016.

Hui, C. S., and W. Chen. 1992b. Effects of conditioning depolarization and repetitive stimulation on Q_β and Q_γ charge components in frog cut twitch fibers. *J. Gen. Physiol.* 99:1017–1043.

Hui, C. S., and W. Chen. 1994a. Evidence for the non-existence of a negative phase in the hump charge movement component (I_γ) in *Rana temporaria*. *J. Physiol.* 474:275–282.

Hui, C. S., and W. Chen. 1994b. Origin of delayed outward ionic current in charge movement traces from frog skeletal muscle. *J. Physiol.* 479:109–125.

Hui, C. S., and W. Chen. 1995. Differential suppression of charge movement components by gluconate in cut twitch fibres of *Rana temporaria*. *J. Physiol.* 489:511–517.

Hui, C. S., and W. Chen. 1997. Charge movement in cut twitch fibres of *Rana temporaria* containing 0.1 mM EGTA. *J. Physiol.* 503:563–570.

Hui, C. S., and J. Maylie. 1991. Multiple actions of 2,3-butanedione monoxime on contractile activation in frog twitch fibres. *J. Physiol.* 442:527–549.

Irving, M., J. Maylie, N. L. Sizto, and W. K. Chandler. 1987. Intrinsic optical and passive electrical properties of cut frog twitch fibers. *J. Gen. Physiol.* 89:1–40.

Janis, R. A., P. J. Silver, and D. J. Triggle. 1987. Drug action and cellular calcium regulation. *Adv. Drug Res.* 16:309–591.

Jong, D. S., P. C. Pape, and W. K. Chandler. 1995. Effect of sarcoplasmic reticulum calcium depletion on intramembranous charge movement in frog cut muscle fibers. *J. Gen. Physiol.* 106:659–704.

Kovacs, L., E. Rios, and M. F. Schneider. 1979. Calcium transients and intramembrane charge movement in skeletal muscle fibres. *Nature.* 279:391–396.

Kovacs, L., E. Rios, and M. F. Schneider. 1983. Measurement and modification of free calcium transients in frog skeletal muscle fibres by a metallochromic indicator dye. *J. Physiol.* 343:161–196.

Malagodi, M. H., and C. Y. Chiou. 1974. Pharmacological evaluation of a new Ca^{++} antagonist, 8-(N,N-Diethylamino)octyl-3,4,5-trimethoxybenzoate hydrochloride (TMB-8): studies in skeletal muscles. *Pharmacology.* 12:20–31.

Maylie, J., and C. S. Hui. 1991. Action of 2,3-butanedione monoxime on calcium signals in frog cut twitch fibres containing antipyrylazo III. *J. Physiol.* 442:551–567.

Maylie, J., M. Irving, N. L. Sizto, and W. K. Chandler. 1987a. Comparison of arsenazo III optical signals in intact and cut frog twitch fibers. *J. Gen. Physiol.* 89:41–81.

Maylie, J., M. Irving, N. L. Sizto, and W. K. Chandler. 1987b. Calcium signals recorded from cut frog twitch fibers containing antipyrylazo III. *J. Gen. Physiol.* 89:83–143.

Melzer, W., M. F. Schneider, B. J. Simon, and G. Szücs. 1986. Intramembrane charge movement and calcium release in frog skeletal muscle. *J. Physiol.* 373:481–511.

Pape, P. C., and N. Carrier. 2002. Calcium release and intramembranous charge movement in frog skeletal muscle fibres with reduced ($<250\ \mu$M) calcium content. *J. Physiol.* 539:253–266.

Pape, P. C., K. Fenelon, and N. Carrier. 2002. Extra activation component of calcium release in frog muscle fibres. *J. Physiol.* 542:867–886.

Pape, P. C., D.-S. Jong, and W. K. Chandler. 1995. Calcium release and its voltage dependence in frog cut muscle fibers equilibrated with 20 mM EGTA. *J. Gen. Physiol.* 106:259–336.

Pape, P. C., D.-S. Jong, and W. K. Chandler. 1996. A slow component of intramembranous charge movement during sarcoplasmic reticulum calcium release in frog cut muscle fibers. *J. Gen. Physiol.* 107:79–101.

Pizarro, G., L. Csernoch, I. Uribe, M. Rodriguez, and E. Rios. 1991. The relationship between Q_γ and Ca release from the sarcoplasmic reticulum in skeletal muscle. *J. Gen. Physiol.* 97:913–947.

Rios, E., and G. Brum. 1987. Involvement of dihydropyridine receptor molecules in excitation-contraction coupling. *Nature.* 325:717–720.

Rios, E., and G. Pizarro. 1988. Voltage sensors and calcium channels of excitation-contraction coupling. *News Physiol. Sci.* 3:223–227.

Shirokova, N., A. González, J. Ma, R. Shirokov, and E. Ríos. 1995. Properties and roles of an intramembranous charge mobilized at high voltages in frog skeletal muscle. *J. Physiol.* 486:385–400.

Shirokova, N., G. Pizarro, and E. Ríos. 1994. A damped oscillation in the intramembranous charge movement and calcium release flux of frog skeletal muscle fibers. *J. Gen. Physiol.* 104:449–477.

Simon, B. J., and D. A. Hill. 1992. Charge movement and SR calcium release in frog skeletal muscle can be related by a Hodgkin-Huxley model with four gating particles. *Biophys. J.* 61:1109–1116.

Squecco, R., C. Bencini, C. Piperio, and F. Francini. 2003. L-type Ca^{2+} channel and ryanodine receptor cross-talk in frog skeletal muscle. *J. Physiol.* 555:137–152.

Vergara, J., and C. Caputo. 1983. Effects of tetracaine on charge movements and calcium signals in frog skeletal muscle fibers. *Proc. Natl. Acad. Sci. USA.* 80:1477–1481.